C4-OH product seen in the microsomal P450s.

Predicted stereoselective product formation from VPA metabolism by $P450_{cam}$ could be checked by performing experiments using VPA as the substrate, with $P450_{cam}$ as the enzyme instead of microsomal P450s. If the results are consistent with those predicted by our calculations, the methods used here to predict the metabolites of $P450_{cam}$ would be validated. We would then conclude that the differences in product distribution between $P450_{cam}$ and microsomal P450 are, in fact, due to specific isozyme differences. These experiments are now in progress.[38]

V. Conclusion

From our calculations of the electronic properties of valproic acid and the protein-substrate interactions of VPA with cytochrome $P450_{cam}$, we have given a reasonable explanation for the observed 4-ene product based upon an initial hydrogen abstraction at the C4 or C4′ positions and made predictions for the site and stereospecificity of the hydroxylated metabolites from $P450_{cam}$. In particular, we have predicted that the metabolites from reaction with $P450_{cam}$ should yield stereospecifically hydroxylated products with C3′-OH + C3-OH > C5′-OH ≥ C4-OH. The predicted product distribution is in contrast to the experimental findings of C4-OH > C3-OH > C5-OH for microsomal P450s, although the stereospecificities of the metabolites of microsomal P450 have not been determined. If our calculated results are correct for $P450_{cam}$, we would have to conclude that the binding sites of $P450_{cam}$ and microsomal P450s are different enough that the product distributions of the hydroxylated metabolites are affected. While the product distribution may be different for the two isozymes, it is possible that the predicted stereoselectivity could be the same.

Our prediction of the absence of the C4′-OH metabolite could be especially significant in the assessment of toxic and teratogenic effects caused by VPA, since the formation of the 4-ene-VPA product could proceed via H abstraction at either the C4 or C4′ positions in the absence of steric constraints. It has been experimentally shown that it is the 4-ene-VPA metabolite that displays liver toxicity[12] and, independently, is known to be a teratogen.[8] More specifically, it has recently been shown that the teratogenicity is due principally to the *S* stereoisomer of 4-ene-VPA.[39] If the C4′-OH is absent as a metabolite of P450, then the teratogenic *S* stereoisomer would not be formed from therapeutically administered VPA, providing an explanation for why metabolites of VPA are apparently not responsible for its teratogenicity.[40] Thus, knowledge of the steric interactions in the binding site of P450 should be useful in designing future drugs with lower toxicity and free of teratogenic consequences by exploiting the possible stereospecificity of P450 metabolism of substrates.

Experiments determining the identity and stereoselectivity of metabolites of VPA using $P450_{cam}$ as the enzyme would test our predictions and guide future theoretical modeling efforts of mammalian cytochrome P450s. In addition, experimental determination of the stereospecificity of the hydroxylated products from the metabolism of VPA by both microsomal P450 and $P450_{cam}$ would further serve as a test of our predicted stereoselectivity and lead to greater insights into the differences between the binding sites of mammalian P450s and $P450_{cam}$ and their detailed interactions with substrates.

Acknowledgment. Support for this work from the Environmental Protection Agency Grant CR-816013-01-0 is gratefully acknowledged.

Registry No. VPA, 99-66-1; 4-ene-VPA, 1575-72-0; C3-OH, 58888-84-9; C4-OH, 60113-82-8; C5-OH, 53660-23-4; cytochrome P450, 9035-51-2; monoxygenase, 9038-14-6.

(38) Baillie, T., private communication.

(39) Nau, H.; Hauck, R.-S. *Toxicol. Lett.* **1989**, *49*, 41-48.
(40) Nau, H. *Fundam. Appl. Toxicol.* **1986**, *6*, 662-668.

Constructing a Molecular Model of the Interaction between Antithrombin III and a Potent Heparin Analogue

Peter D. J. Grootenhuis* and Constant A. A. van Boeckel*

Contribution from the Akzo Pharma Division, Organon Scientific Development Group, P.O. Box 20, 5340 BH Oss, The Netherlands. *Received August 14, 1990*

Abstract: Information about the antithrombin III-heparin interaction is deduced from the following: (i) structure-activity studies of various synthetic analogues of the antithrombin III binding pentasaccharide domain of heparin, which revealed that essential sulfate and carboxylate substituents are located at opposite sides of the pentasaccharide molecule; (ii) studies that designated the heparin-binding amino acid residues of antithrombin III; (iii) a molecular model of antithrombin III, constructed on the basis of the crystal structure of α1-antitrypsin. From these studies it could be deduced that *both* the protein and the carbohydrate display an asymmetric assembly of essential interaction points. Docking trials indicated a single complex in which the interaction points are complementary. The latter complex was optimized by molecular dynamics simulations. The final model reveals, for the first time, how a well-defined region of a sulfated polysaccharide can interact specifically with a complementary binding site on a functional protein.

Although it has been recognized that interactions among sulfated polysaccharides (glycosaminoglycans) and proteins are involved in cellular adhesion and various physiological processes, only the heparin-antithrombin III (AT-III) system has been studied at the molecular level.[1] A major breakthrough was the finding that only part of the sulfated polysaccharides[2,3] of the anticoagulant drug heparin displays high affinity to AT-III. Subsequently, it was discovered that this part of the heparin polysaccharides contains a well-defined pentasaccharide region[4,5] that specifically binds and activates the protease inhibitor AT-III.

* Author to whom correspondence should be addressed.

(1) *Heparin, Chemical and Biological Properties, Clinical Applications*; Lane, D. A., Lindahl, V., Eds.; Edward Arnold: London, 1989.
(2) Lam, L. H.; Silbert, J. E.; Rosenberg, R. D. *Biochem. Biophys. Res. Commun.* **1976**, *69*, 570-577.
(3) Höök, M.; Björk, I.; Hopwood, J.; Lindahl, U. *FEBS Lett.* **1976**, *66*, 90-93.
(4) Choay, J.; Lormeau, J. C.; Petitou, M.; Sinay, P.; Fareed, J. *Ann. N.Y. Acad. Sci.* **1981**, *370*, 644-649.

0002-7863/91/1513-2743$02.50/0

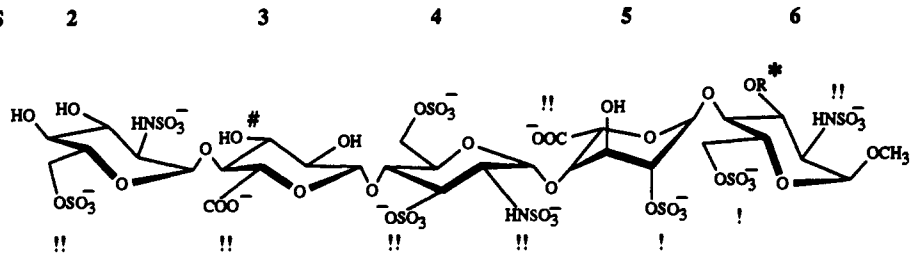

Ia : R = H

Ib : R = SO_3^-

Figure 1. Structure–activity relationships of heparin-like pentasaccharide analogues that activate AT-III. By comparison of the AT-III-mediated αXa activities[40] of compound Ia[39] (740 αXa units/mg) with that of other synthetic pentasaccharides it has been established which charged groups of the pentasaccharide are essential for optimal interaction with AT-III. The sulfate and carboxylate groups indicated with exclamation marks are critical since their removal leads to more than 95% (!!) or ~75% (!) loss of αXa activity. Introduction of an extra 3-*O*-SO_3^- group (*) at unit 6 leads to compound Ib (Org 31550), being the most potent analogue (1270 αXa units/mg) found thus far.[20,21] Introduction of extra sulfate groups at unit 2 of Ib leads to analogues with similar biological activity,[33] whereas substitution of an extra 3-*O*-SO_3^- group at unit 3 of Ib (#) provides a less potent analogue displaying only 480 αXa units/mg.[33] Replacement of the aminosulfate group at unit 2 of Ib by a hydroxyl group provides a slightly less active analogue (844 αXa units/mg).

Thus, the paradigm was contradicted that the biological activity of heparin was due to its polyanionic character mainly. The specific pentasaccharide fragment of heparin induces a conformational change in AT-III, thereby accelerating the AT-III-mediated inactivation of blood coagulation factor Xa.[6,7] By selective processing of isolated heparin fragments[8-10] and through organic synthesis[11-15] of pentasaccharide analogues, it became clear that for AT-III activation the presence and spatial orientation of particular carboxylate and sulfate groups of the pentasaccharide is important (Figure 1), as well as the presence of the rigid carbohydrate moieties.[16] Most likely the essential charged groups of the pentasaccharide interact with complementary lysine and arginine residues at the surface of AT-III.

Conformational analysis of some synthetic heparin fragments[17-19] provided information on the spatial orientation of the charged groups of the pentasaccharide. Since it was observed that the essential groups are located on opposite sides ("south and north") of the carbohydrate, we contemplated[15a] that the pentasaccharide would interact through a two-sided binding with the protein. This hypothesis was corroborated by the synthesis[20,21] of the analogue Ib (Figure 1) which contains at unit 6 an extra 3-O sulfate group that may interact with the tentative AT-III binding site at the north side of the pentasaccharide. Compound Ib is known to be the most potent catalyst in the AT-III directed inhibition of factor Xa.[20,21] In Figure 1 it can be seen that six charged groups of Ib, which span monosaccharide units 2–6, define an extended binding area at the south of the molecule. At the north of the molecule a smaller binding area is expected to be present, consisting of three charged groups at units 5 and 6. This asymmetrical assembly of interaction points turned out to be crucial for determining the orientation of Ib toward the complementary protein binding sites. In the present paper, we describe initial results of model building and molecular dynamics (MD) studies that provide insight into the interaction between pentasaccharide Ib and AT-III at the molecular level.

Computational Methods

All model building, docking, energy minimization, and molecular dynamics studies were carried out using Quanta/CHARMm version 2.1A (Polygen Corp., Waltham, MA, August 1989). The simulations were performed on a Silicon Graphics 4D/120GTX workstation equipped with a stereo graphics facility.

Homology Model Building. A three-dimensional model structure of residues 45–431 of human AT-III was constructed by using the atomic coordinates from the crystal structure of human α1-antitrypsin[22] (Brookhaven Protein Data Bank code 5API). The sequence alignment (and amino acid numbering) for the serpin family published by Huber and Carrell[23] could be employed as a basis for the homology model building procedure. In this alignment, the overall homology (based on identical residues) between AT-III and α1-antitrypsin amounts to 28%; if structural similarity among amino acids was considered, the homology between the two proteins would increase significantly. The amino acid substitutions, insertions, and deletions were all made by using the tools and default amino acid geometries present in the Protein Module of Quanta/CHARMm. Reasonable conformations for the backbones of the amino acid residues that had to be inserted were taken from a database containing 50 protein crystal structures selected from the Protein Data Bank. It was determined that the disulfide bond between Cys 247 and

(5) Thunberg, L.; Bäckström, G.; Lindahl, U. *Carbohydr. Res.* **1982**, *100*, 393–410.
(6) Atha, D. H.; Lormeau, J. C.; Petitou, M.; Rosenberg, R. D.; Choay, J. *Biochemistry* **1985**, *24*, 6723–6729.
(7) Choay, J.; Petitou, M.; Lormeau, J. C.; Sinay, P.; Casu, B.; Gatti, G. *Biochem. Biophys. Res. Commun.* **1983**, *116*, 492–499.
(8) Riesenfeld, J.; Thunberg, L.; Höök, M.; Lindahl, U. *J. Biol. Chem.* **1981**, *256*, 2389–2394.
(9) Lindahl. U.; Bäckström, G.; Thunberg, L. *J. Biol. Chem.* **1983**, *258*, 9826–9830.
(10) Otatani, N.; Kikuchi, M.; Yosizawa, Z. *Biochem. J.* **1982**, *205*, 23–30.
(11) (a) Sinay, P.; Jacquinet, J. C.; Petitou, M.; Duchaussoy, P.; Lederman, I.; Choay, J.; Torri, G. *Carbohydr. Res.* **1984**, *132*, C5–C9. (b) van Boeckel, C. A. A.; Beetz, T.; Vos, J. N.; de Jong, A. J. M.; van Aelst, S. F.; van der Bosch, R. H.; Mertens, J. M. R.; van der Vlugt, F. A. *J. Carbohydr. Chem.* **1985**, *4*, 293–321.
(12) Petitou, M. *Nouv. Rev. Fr. Hematol.* **1984**, *26*, 221–226.
(13) Petitou, M.; Lormeau, J. C.; Choay, J. *Eur. J. Biochem.* **1988**, *88*, 637–640.
(14) Beetz, T.: van Boeckel, C. A. A. *Tetrahedron Lett.* **1986**, *27*, 5889–5892.
(15) (a) van Boeckel, C. A. A.; Lucas, H.; van Aelst, S. F.; van den Nieuwenhof, M. W. P.; Wagenaars, G. N.; Mellema, J.-R. *Recl. Trav. Chim. Pays-Bas* **1987**, *106*, 581–591. (b) van Aelst, S. F.; van Boeckel, C. A. A. *Recl. Trav. Chim. Pays-Bas* **1987**, *106*, 593–595.
(16) (a) van Boeckel. C. A. A.; Basten, J. E. M.; Lucas, H.; van Aelst, S. F. *Angew. Chem.* **1988**, *100*, 1217–1219. (b) Lucas, H.; Basten, J. E. M.: van Dinther, Th. G.; Meuleman, D. G.; van Aelst, S. F.; van Boeckel, C. A. A. *Tetrahedron* **1990**, *46*, 8207–8228.
(17) Ferro, D. R.; Provasoli, A.; Ragazzi, M.; Torri, G.; Casu, B.; Gatti, G.; Jacquinet, J. C.; Sinay, P.; Petitou, M.; Choay, J. *J. Am. Chem. Soc.* **1986**, *108*. 6773–6778.
(18) Ragazzi, M.; Ferro, D. R.; Perly, B.; Torri, G.; Casu, B.; Sinay, P.; Petitou, M.: Choay, J. *Carbohydr. Res.* **1987**, *165*, C1–C5.
(19) van Boeckel, C. A. A.; van Aelst, S. F.; Wagenaars, G. N.; Mellema, J.-R.; Paulsen, M.: Peters, T.; Pollex, A.; Sinnwell, V. *Recl. Trav. Chim. Pays-Bas* **1987**, *106*, 19–29.
(20) van Boeckel, C. A. A.: Beetz, T.; van Aelst, S. F. *Tetrahedron Lett.* **1988**, *29*, 803–806.
(21) van Boeckel, C. A. A.; van Aelst, S. F.; Beetz, T.; Meuleman, D. G.; van Dinther, Th. G.; Moelker, H. C. T. *Ann. N.Y. Acad. Sci.* **1989**, *556*, 489–491.
(22) Löbermann, H.; Tokuoka, R.: Deisenhofer, J.; Huber, R. *J. Mol. Biol.* **1984**, *177*, 531–556.
(23) Huber, R.; Carrell, R. W. *Biochemistry* **1989**, *28*, 8952–8966.

Cys 430 was present. It should be noted that in the present model the N-glycoconjugate fragments of the glycoprotein were not included and furthermore that at the N-terminal residue 45 a formamide group (using the NFRM patch) was attached to mimic a peptide bond at this position. Bad nonbonded contacts originating from side chains of amino acid residues bumping into each other were partially removed by manually adjusting the side-chain torsional angles. The structure thus obtained was further optimized by constrained energy minimization. The positional harmonic constraints were gradually removed from the backbone atoms while the structure was subjected to molecular mechanics optimization. The root mean square (rms) deviation for the α-carbon atoms between the initial and the energy-minimized structure amounted to 1.15 Å.

Molecular Mechanics and Dynamics. Throughout all the calculations, unless noted otherwise, default values for the various CHARMm molecular mechanics and dynamics parameters were taken. A distance-dependent dielectric constant in combination with a 12-Å nonbonded cutoff was maintained. The polar hydrogen atom description of the amino acids of AT-III as implemented in the AMINO.RTF file was used (hydrogens bound to carbon not represented explicitly); however, for the pentasaccharide the all-atom force field was used. Conjugate gradient energy minimizations were continued until the rms energy gradient was less than 0.25 kcal/mol·Å.

The initial structure of pentasaccharide Ib, derived from conformational analysis studies, was energy-minimized and subsequently docked on the AT-III model structure in an orientation inspired by the principal complementarity of the interaction points of the protein and pentasaccharide (vide infra). The bonded and nonbonded sulfate parameters that are not available from the CHARMm parameter set (PARM21A.PRM) will be published elsewhere. The complex was energy-minimized and then relaxed by a 5-ps MD run. A constant temperature of 300 K was maintained during the run by velocity scaling. All residues within 20 Å of the pentasaccharide were permitted to move during the course of the MD simulations, while the remaining residues were held fixed. A time step of 0.001 ps was used. The nonbonded pair list was updated every 50 time steps.

The pentasaccharide in the structure after 5 ps of MD was then hydrated by a 10-Å shell of (TIP3P) water molecules. Water molecules that came to close to an AT-III atom were removed. A positional harmonic constraint of 0.1 kcal/mol·Å was applied to the water oxygens to prevent evaporation. The system was composed of 3941 protein and carbohydrate atoms and 183 water molecules for a total of 4490 atoms. Finally, a 30-ps MD run at 300 K was carried out. The coordinates of all atoms were saved every 0.1 ps for future analysis. The final structure after 30 ps of MD was energy-minimized and analyzed. The rms deviation for the α-carbon atoms between this structure and the initial model-built structure was 1.54 Å.

Results and Discussion

Since no crystal structure of AT-III is available, we had to resort to the crystal structure of cleaved α1-antitrypsin[22] on which, according to Huber and Carrell,[23,24] the AT-III heparin binding site may be projected. By standard homology model building techniques[25] we constructed a three-dimensional model of residues 45–431 of human AT-III. As a starting point for the docking of pentasaccharide Ib on AT-III we focused on the positively charged amino acid residues Arg 46, Arg 47 (both at the top of helix A); Lys 125, Arg 129, Arg 132, Lys 133, Lys 136 (all part of helix D); Lys 107 and Lys 114. This selection is based on data originating from modified AT-III derivatives displaying decreased heparin affinity,[26-30] the fact that the region 123–141 possesses the highest positive charge density,[31] and reports showing that residues 41–49 are essential for the heparin-enhanced activity of AT-III.[26,27,32] Since *both* the carbohydrate and the protein expose

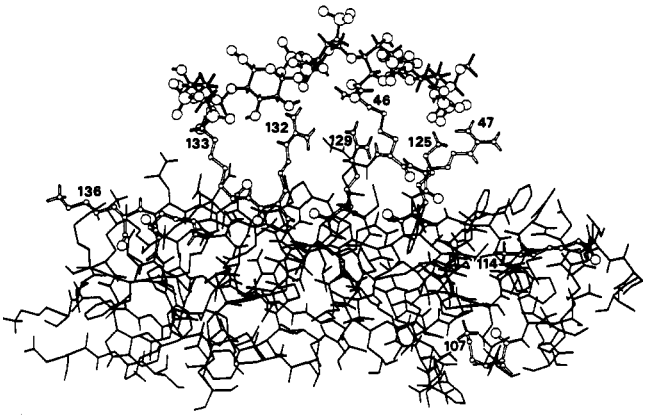

Figure 2. Side view of the docked AT-III·Ib complex, showing Arg and Lys residues 46, 47, 125, 129, 132, 133, 136, 107, and 114 by using open bonds and Ib as a ball–stick model. For clarity only the residues within 20 Å of Ib are displayed. Clearly, residues 107, 114, and 136 are initially not in close proximity to the tentative pentasaccharide binding site; during MD only Lys 136 reoriented itself to interact with the pentasaccharide.

an asymmetrical assembly of interaction points, their orientation toward each other could be established during docking trials. The docked structure displaying the most favorable interaction energy between the protein and the pentasaccharide—as calculated after 5 ps of MD simulation—was that one in which residues Lys 125, Arg 129, Arg 132, and Lys 133 form an elongated, positively charged binding site complementary to the negatively charged southern region of pentasaccharide Ib, leaving Arg 46 and Arg 47 in an appropriate position to interact with the northern charged groups of units 5 and 6 of Ib (see Figure 2).

The docked structure was energy-minimized and then relaxed by a 5-ps MD run to establish many bonding interactions among oppositely charged groups. It should be noted that for the flexible iduronic acid moiety of Ib[17-19] we used the $^1C_4$ conformation as a starting geometry. This choice is based on the observation that the $^1C_4$ conformation of iduronic acid is more energetically favorable at high ionic conditions, although the $^2S_0$ conformation dominates under low ionic conditions.[17-19] (An alternative MD run that was started with the iduronic acid moiety of the pentasaccharide in the $^2S_0$ conformation resulted in a complex with an interaction energy between the protein and the pentasaccharide ±20 kcal/mol less favorable than in the corresponding complex of the original run in which the $^1C_4$ conformation is present.) Although the overall orientation of the pentasaccharide toward the two protein binding sites is maintained during the 5-ps MD simulation, quite remarkably the initially distant Lys 275 residue moved toward the sulfamino group at unit 2 (Figure 2). In this respect it is noteworthy that a synthetic analogue containing a hydroxyl group instead of a sulfamino group in this position loses ~30% of its biological activity.[33] Since ordered water molecules may influence the protein–carbohydrate interaction,[34] the 5-ps structure was partly hydrated and subjected to 30 ps of MD at 300 K. The final structure after 30 ps of MD was energy-minimized and is depicted in Figure 3.

During the first 5 ps of the latter MD simulation, Lys 136, known to be directly involved in heparin binding,[30] approaches the essential 6-*O*-sulfate at unit 2. The model explains the favorable contributions of essential (amino)sulfate and carboxylate groups of the potent synthetic heparin fragment (Ib) to the binding with AT-III. The observation that the introduction of an extra sulfate group at the 3-O position of unit 3 of compound Ib leads to a 65% loss of biological activity,[33] can be ascribed to the electrostatic repulsion of the latter sulfate group with Asp 278.

The higher activity of Ib with respect to Ia can be explained in our model by the extra interaction of the 3-*O*-sulfate in unit 6 with Arg 46 of the northern binding site.

(24) Borg, J. Y.; Owen, M. C.; Soria, C.; Caen, J.; Carrell. R. W. *J. Clin. Invest.* **1988**, *81*, 1292–1296.
(25) (a) Blundell, T. L.; Sibanda, B. L.; Sternberg, M. J. E.; Thornthon, J. M. *Nature* **1987**, *326*, 347–352. (b) Greer, J. *Proteins* **1990**, *7*, 317–334.
(26) Koide, T.; Odani, S.; Tokahashi, K.; Ono, T.; Sakuragawa. N. *Proc. Natl. Acad. Sci. U.S.A.* **1984**, *81*, 289–293.
(27) Owen, M. C.; Borg, J. Y.; Soria, C.; Soria, J.; Caen, J.; Carrell, R. W. *Blood* **1987**. *69*. 1275–1279.
(28) Liu, C.-S.; Chang, J.-Y. *J. Biol. Chem.* **1987**, *262*, 17356–17361.
(29) Peterson, C. B.; Noyes, C. M.; Pecon, J. M.; Church, F. C.; Blackburn, M. N. *J. Biol. Chem.* **1987**, *262*, 8061–8065.
(30) Chang, J.-Y. *J. Biol. Chem.* **1989**, *264*, 3111–3115.
(31) Smith, J. W.; Knauer, J. *J. Biol. Chem.* **1987**, *262*, 11964–11972.
(32) Blackburn, M. N.; Smith, R. C.; Carson, J.; Sibley. C. C. *J. Biol. Chem.* **1984**, *259*. 939–941.
(33) van Boeckel, C. A. A., presented at EUROCARB V, Prague, August 21–25, 1989.
(34) Quiocho, F. A. *Pure Appl. Chem.* **1989**, *61*, 1293–1306.

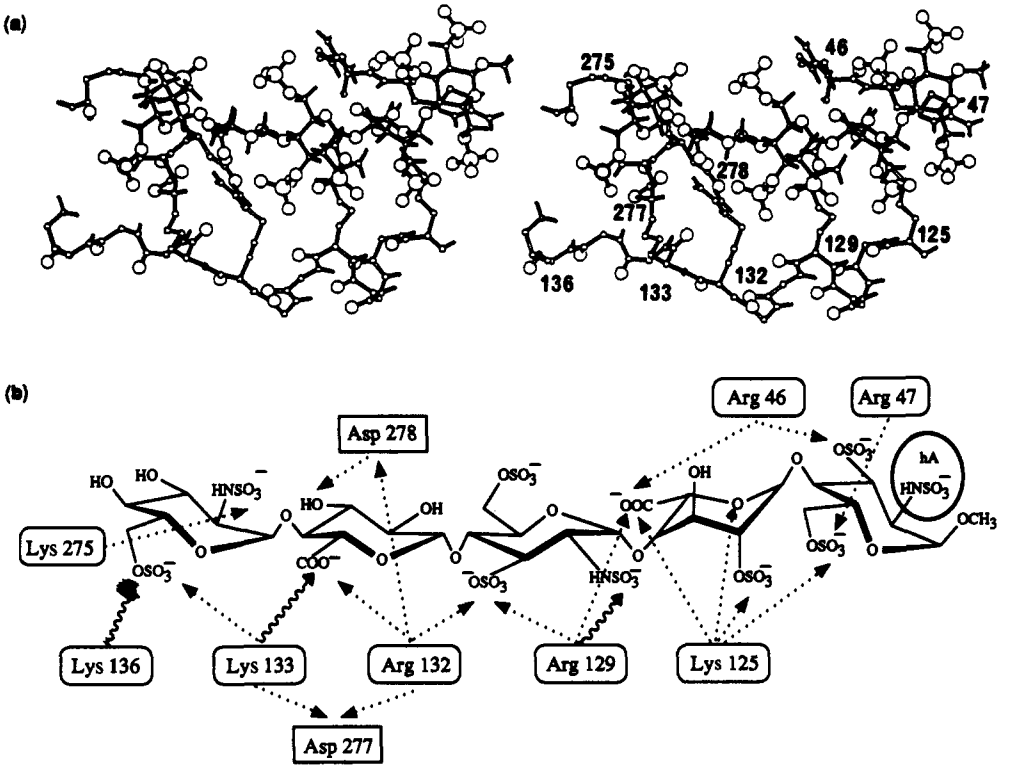

Figure 3. (a) Stereoplot of the interaction area of the energy-minimized final structure of the AT-III·Ib complex after 5-ps gas-phase MD followed by 30 ps of MD in the presence of water molecules. For clarity water molecules are not shown. The amino acids are depicted by use of open bonds while solid bonds are used for Ib. (b) Schematic diagram of the hydrogen-bonding network (---> denotes directly hydrogen bonds, while ~~> denotes hydrogen bond arrays through ordered water molecules) in the AT-III·Ib complex as present in the energy-minimized structure after 30 ps of MD. The ellipse denotes the approximate position of the N terminus of helix A of AT-III (hA), oriented perpendicularly to the pentasaccharide.

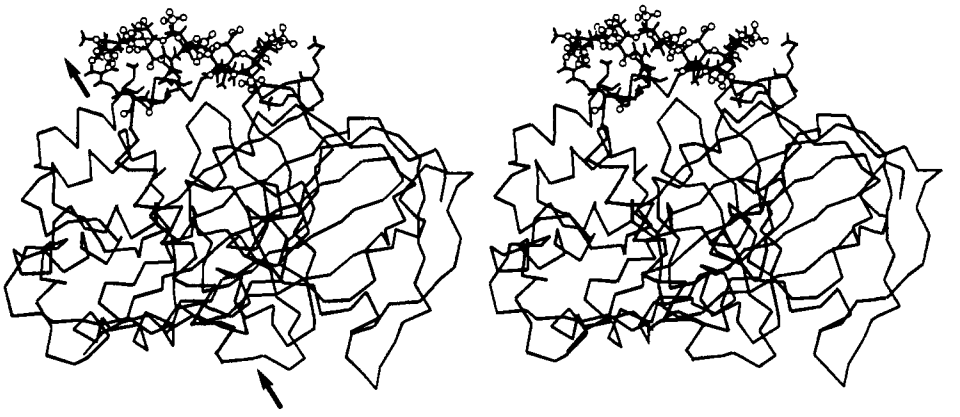

Figure 4. α-Carbon stereoplot of the AT-III·Ib complex. Helix A is displayed by using solid lines while Ib is depicted as a ball–stick model. Only the side chains of the interacting amino acids are shown. The arrows indicate the direction of the helix dipole of helix A.

The presence of two separate binding sites in this model is in agreement with kinetic studies revealing that binding of heparin to AT-III should be interpreted as a two-step process.[35,36] In our view, the first step in the binding process is the interaction of the southern side of the pentasaccharide with amino acids 125, 129, 132, 133, and 136 positioned at helix D. The second step should involve the well-studied conformational change of AT-III,[37] known to substantially contribute to the heparin binding. This step can be conceived as an induced fit between the northern side of the pentasaccharide and the residues Arg 46 and Arg 47 at the top of helix A of AT-III. Furthermore, the exact location of the aminosulfate residue at unit 6 in the field of the dipole of the N-terminal helix A (see Figure 4) not only enhances the interaction with AT-III,[6,38] but also suggests the participation of this helix in the transmission of the conformational change in the heparin binding site toward the protease inhibition site in AT-III (Arg 393).

Conclusion

The present molecular model based on (i) structure–activity relationships of pentasaccharide analogues, (ii) knowledge of essential heparin-binding amino acid residues on AT-III, (iii) the

(35) Olson, S. T.; Srinivasan, K. R.; Björk, I.; Shore, J. D. *J. Biol. Chem.* **1981**, *256*, 11073–11079.
(36) Craig, P. A.; Olson, S. T.; Shore, J. D. *J. Biol. Chem.* **1989**, *264*, 5452–5461.
(37) Villanueva, G. B.; Danishefsky, I. *Biochem. Biophys. Res. Commun.* **1977**, *74*, 803–809.
(38) (a) Hol, W. G. J.; van Duijnen, P. T.; Berendsen, H. J. C. *Nature* **1978**, *273*, 443–446. (b) Hol, W. G. J. *Prog. Biophys. Mol. Biol.* **1985**, *45*, 149–195.
(39) Petitou, M.; Duchaussoy, P.; Lederman, I.; Choay, J.; Jacquinet, J. C.; Sinay, P.; Torri, G. *Carbohydr. Res.* **1987**, *167*, 67.
(40) In an amidolytic assay in plasma with chromogenic substrate S222 the anti-factor Xa (αXa) activity is measured: Teien, A. N.; Lie, M.; Albidgaard, U. *Thromb. Res.* **1976**, *8*, 413–416.

crystal structure of the homologous α1-antitrypsin, and (iv) molecular dynamics simulations provides for the first time detailed insight in the *highly specific* binding of a sulfated polysaccharide (glycosaminoglycan) fragment with a protein at the molecular level. We feel that specific binding of other proteins with sulfated polysaccharides may also involve well-defined, relatively small complementary domains on both the carbohydrate polymer and the protein.

Acknowledgment. We thank Dr. Kees Haasnoot (Organon SDG) and Dr. Maurice Petitou (Sanofi Recherche, Paris, France) for useful discussions and Mr. Theo van Dinther (Organon SDG) for determining the αXa activities.

Registry No. AT-III, 9000-94-6; heparin, 9005-49-6.

Nature of the Epoxidizing Species Generated by Reaction of Alkyl Hydroperoxides with Iron(III) Porphyrins. Oxidations of *cis*-Stilbene and (*Z*)-1,2-Bis(*trans*-2,*trans*-3-diphenylcyclopropyl)ethene by *t*-BuOOH in the Presence of [*meso*-Tetrakis(2,4,6-trimethylphenyl)porphinato]-, [*meso*-Tetrakis(2,6-dichlorophenyl)porphinato]-, and [*meso*-Tetrakis(2,6-dibromophenyl)porphinato]iron(III) Chloride

Gong-Xin He and Thomas C. Bruice*

Contribution from the Department of Chemistry, University of California at Santa Barbara. Santa Barbara, California 93106. *Received August 30, 1990*

Abstract: The mechanism of the oxidation of alkenes by *t*-BuOOH in the presence of iron(III) tetraphenylporphyrins has been explored (CH_2Cl_2 sovent). The alkenes, *cis*-stilbene and (*Z*)-1,2-bis(*trans*-2,*trans*-3-diphenylcyclopropyl)ethene (**1**-*Z*), have been chosen because they serve as traps for radical intermediates. The substituted iron(III) tetraphenylporphyrin catalysts employed are [*meso*-tetrakis(2,4,6-trimethylphenyl)porphinato]iron(III) chloride ((TMP)Fe^{III}(Cl)), [*meso*-tetrakis(2,6-dichlorophenyl)porphinato]iron(III) chloride ((Cl_8TPP)Fe^{III}(Cl)), and [*meso*-tetrakis(2,6-dibromophenyl)porphinato]iron(III) chloride ((Br_8TPP)Fe^{III}(Cl)). In separate experiments, azobisisobutyronitrile (AIBN) was used as a radical chain initiator for the oxidation of the alkenes by *t*-BuOOH. Oxidation of *cis*-stilbene with iron(III) porphyrins as catalysts provides *trans*-stilbene oxide as a major product along with diphenylacetaldehyde, deoxybenzoin (trace), and a compound assigned [^{1}H NMR, MS(CI)] the structure PhCH[OO(*t*-Bu)]CH[O(*t*-Bu)]Ph. We conclude that the reaction products are derived from initial combination of *t*-BuOO$^\cdot$, rather than ($^{+\cdot}$Porph)Fe^{IV}(O), with *cis*-stilbene. Oxidation of **1**-*Z* with iron(III) porphyrins as catalysts provides A (^{1}H NMR, MS(CI), FT-IR) as the major product. Other products are B (whose structure has not been determined), which contains intact one of the two *trans*-2,*trans*-3-diphenylcyclopropane groups, *trans*-2,*trans*-3-diphenylcyclopropanecarboxaldehyde, and deoxybenzoin. In A, one cyclopropyl group has undergone a cyclopropylcarbinyl to homoallylcarbinyl radical rearrangement (CPCRR) while the other has remained intact. The major product A arises from initial combination of *t*-BuOO$^\cdot$ with **1**-*Z* followed by CPCRR. Reaction sequences are suggested. The *cis*-epoxide of **1**-*Z* (**2**-*c*) is formed in 3.2% yield when (Cl_8TPP)Fe^{III}(Cl) is the catalyst. A trace of **2**-*c* is obtained with (TMP)Fe^{III}(Cl), but **2**-*c* could not be detected with (Br_8TPP)Fe^{III}(Cl). The *cis*-epoxide **2**-*c* most likely arises from the concerted reaction of **1**-*Z* with the iron(IV)–oxo porphyrin π cation radical ($^{+\cdot}Cl_8$TPP)Fe^{IV}(O)(Cl). The species ($^{+\cdot}Cl_8$TPP)Fe^{IV}(O)(Cl) may be the direct product of reaction of (Cl_8TPP)Fe^{III}(Cl) with *t*-BuOOH in a mechanism that involves heterolytic O–O bond breaking. Alternatively, ($^{+\cdot}Cl_8$TPP)Fe^{IV}(O)(Cl) may arise via (Cl_8TPP)Fe^{III}(Cl) + *t*-BuOOH → (Cl_8TPP)Fe^{IV}(O) + *t*-BuO$^\cdot$ followed by oxidation of (Cl_8TPP)Fe^{IV}(O) by *t*-BuOOH (or other). It is pointed out that (Cl_8TPP)Fe^{IV}(O), unlike (TMP)Fe^{IV}(O), accumulates in relatively high concentration and that *t*-BuOOH is present at 0.3 M.

Introduction

Iron(III) porphyrins have been established as effective catalysts for the epoxidation of norbornene (Nb) with *t*-BuOOH at high concentrations of alkene.[1,2] Epoxidation has been proposed to involve the reactions of eqs 1 and 2.[1] The mechanism of the

$$t\text{-BuOOH} + (\text{Porph})Fe^{III}(X) \rightarrow t\text{-BuOH} + (^{+\cdot}\text{Porph})Fe^{IV}(O)(X) \quad (1)$$

$$(^{+\cdot}\text{Porph})Fe(O)(X) + Nb \rightarrow (\text{Porph})Fe^{III}(X) + \textit{endo}\text{-NbO}/\textit{exo}\text{-NbO} \quad (2)$$

reaction of eq 1 is suggested to involve an intermediate complex of iron(III) porphyrin and hydroperoxide that decomposes to products with O–O bond heterolysis and oxygen transfer to iron(III) porphyrin accompanied by its 2e$^-$ oxidation. The ratio of *endo*- to *exo*-norbornene epoxides (NbO) has been interpreted as showing that the epoxidations are carried out by a

(1) (a) Traylor, T. G.; Xu, F. *J. Am. Chem. Soc.* **1987**, *109*, 6201. (b) Traylor, T. G.; Fann, W-P.; Bandyopadyay, D. *J. Am. Chem. Soc.* **1989**, *111*, 8009.

(2) We have repeated Traylor's study with norbornene and found that we obtained similar yields of epoxide under the same conditions.

0002-7863/91/1513-2747$02.50/0